Pharm Res (2015) 32:469–481
DOI 10.1007/s11095-014-1475-3

RESEARCH PAPER

Nanomechanical Properties of Selected Single Pharmaceutical Crystals as a Predictor of Their Bulk Behaviour

Mateja Egart • Biljana Janković • Nina Lah • Ilija Ilić • Stanko Srčič

Received: 9 February 2014 / Accepted: 25 July 2014 / Published online: 5 August 2014

ABSTRACT

Purpose The main goal of this research was to assess the mechanical properties of APIs' polymorphic forms at the single-crystal level (piroxicam, famotidine, nifedipine, olanzapine) in order to predict their bulk deformational attributes, which are critical for some pharmaceutical technology processes.

Methods The mechanical properties of oriented single crystals were determined using instrumented nanoindentation (continuous stiffness measurement). All polymorphic forms investigated were previously identified using a combination of calorimetric and spectroscopic techniques.

Results Mechanical properties such as Young's modulus and indentation hardness were consistent with the molecular packing of the polymorphic forms investigated with respect to crystal orientation. For mechanically interlocked structures, characteristic of most polymorphic forms, response of single crystals to indentation was isotropic. The material's bulk elastic properties can be successfully predicted by measuring Young's modulus of single crystals because a good linear correlation with a bulk parameter such as the tablets' elastic relaxation index was determined.

Conclusions The results confirm the idea that the intrinsic mechanical properties of pharmaceutical crystals (Young's modulus) largely control and anticipate their deformational behavior during tablet compression. Young's modulus and indentation hardness represent a very valuable and effective tool in preformulation studies for describing materials' mechanical attributes, which are important for technological processes in which materials are exposed to deformation.

M. Egart • B. Janković (✉) • I. Ilić • S. Srčič
Department of Pharmaceutical Technology, Faculty of Pharmacy
Aškerčeva 7, 1000 Ljubljana, Slovenia
e-mail: biljana.jankovic@ffa.uni-lj.si

N. Lah
Faculty of Chemistry and Chemical Technology Aškerčeva 7,
1000 Ljubljana, Slovenia

KEY WORDS Single crystal · Crystallography · Instrumented nanoindentation · Crystal mechanical properties · Bulk mechanical properties

INTRODUCTION

The mechanical behavior of molecular solids is unique in comparison to extended solids because the structures are stabilized by weak interactions (hydrogen bonds and van der Waals interactions) and also due to their characteristic structural anisotropy. Despite the influence that mechanical properties have on industrial-scale production and handling, their evaluation and assessment for pharmaceutical materials is still uncommon today [1]. The mechanical behavior of crystalline solids depends on the types and strengths of bonds among the molecules, their packaging, and any lattice defects that may be present. The types and distribution of defects have a significant impact on the plasticity and brittleness specific for crystals and their aggregates [2, 3].

Here we used a method for measuring mechanical properties of pharmaceutical ingredients (API and excipients) called instrumented nanoindentation. The method is a common approach for determining deformational properties of materials in metallurgy, although it is gradually becoming applied in pharmaceutical materials science, where processing events in industry involve mechanical operations (e.g., milling or compression) [4–9]. Therefore, understanding the mechanical performance of molecular crystals in the context of crystal packing, slip, and defects is not only of scientific significance but also of practical importance.

Under mechanical stress, pharmaceutical materials usually undergo elastic and plastic deformation and/or fragmentation. Elastic deformation is a consequence of weak intermolecular forces among molecules (mostly van der Waals interactions and hydrogen bonding) due to which pharmaceutical materials are classified as soft materials with low elastic moduli [10].

Generally, fragmentation improves consolidation (by tableting or compacting); however, compacts containing

brittle materials demonstrate the tendency of capping or lamination (during the decompression phase). Crystal fracture occurs when the shear stress reaches a level at which dislocation pile-up attains a critical density. Some materials can also fracture along specific crystal planes by cleavage where the surface energy is the lowest [10].

Adequate compaction properties of any given powder material are largely a function of material plasticity, which increases the contact area and bonding between particles [11, 12].

The plastic deformation of crystals is expected to take place on low-index slip planes, which can be identified with higher in-plane molecular density accompanied by weak inter-planar interactions and lower molecular rugosity.

Besides nanoindentation, intensive compressibility studies of the crystalline materials can be performed with hydrostatic compression as well as high pressure diffraction approaches [13–16]. Under high pressure, anisotropy of the crystals can be investigated with respect to intermolecular interactions as well as correlations between lattice strain or interatomic distances and applied pressure. For instance, polymorphic forms of paracetamol have the same bulk compressibility, but it is the anisotropy of strain that differs. For orthorhombic form of paracetamol, isotropic compressibility of crystal layers is characteristic whereas for monoclinic layers are expanded in some directions and compressed in the other. These observations can be quantitatively described with changes in intermolecular bond lengths and modifications in the dihedral and torsion angles in respect to applied pressure [13, 14]. Therefore, our main goal was to assess the mechanical properties of APIs' polymorphic forms at the single-crystal level and to compare them with bulk deformational properties. Mechanical behavior of the powder bed during compression will be used for evaluation of so-called bulk mechanical properties. Pharmaceutical crystalline materials are extensively studied in terms of the crystallization process and controlling it, determining and predicting crystal structures, and their surface properties. However, quantitative understanding of the mechanical properties of structurally known molecular crystals (intensively used in the pharmaceutical industry) remains uncommon. This knowledge gap has an apparent impact in applications in which crystalline APIs are subject to mechanical stresses (e.g., compression and milling).

Finally, we would like to highlight all the practical aspects of the nanoindentation method and to estimate its reliability and the reproducibility of measuring fundamental properties of pharmaceutical materials such as deformational attributes.

As a strategy, several common APIs such as piroxicam, famotidine, olanzapine, and nifedipine were taken into consideration. At the initial stage, their deformational characteristics were not known from the literature data. From the practical point of view, only thermodynamically stable forms were used, oriented and mechanically characterized at the single-crystal and the bulk level. An exception was famotidine, in which both polymorphs, A (thermodynamically most stable) and B (the kinetically favored form), were included in the study. The polymorph of famotidine commercialized on the market is form B, which demonstrates higher activity and a higher dissolution rate in comparison to form A [17].

MATERIALS AND METHODS

Materials

Piroxicam, famotidine, nifedipine, and olanzapine were obtained on the local market in Slovenia. 1-butyl-3-methylimidazolium tetrafluoroborate (Merck, Darmstadt, Germany) was used as a crystallization additive for producing large single crystals. For preparing crystallization media, analytical grade solvents were used: acetonitrile, methanol, benzyl alcohol, ethyl acetate, and acetone were supplied by Merck (Darmstadt, Germany).

Preparation of the Polymorphic Forms

Piroxicam Polymorphic Form I

We added 500 mg of piroxicam to 10 mL of benzyl alcohol. The mixture was slowly heated to boiling temperature (~205°C) and refluxed for 30 min. The hot solution was filtered and the filtrate left at ambient conditions to slowly evaporate the solvent. Colorless prismatic and rod-like shaped crystals of the β-form appeared after 1 day [18].

Famotidine Polymorphic Form A

We added 200 mg of famotidine to 50 mL of acetonitrile. The mixture was slowly heated to boiling temperature (~81°C) and refluxed for 2 h. The hot solution was filtered and the filtrate left at ambient conditions to slowly evaporate the solvent. Colorless rectangular prismatic crystals appeared after a few hours [19].

Famotidine Polymorphic Form B

We dissolved 150 mg of famotidine powder in a mixture of 8 ml of methanol and 2 ml of acetone. Large single crystals were obtained by adding 300 μl of ionic liquid, 1-butyl-3-methylimidazolium tetrafluoroborate. The mixture was slowly heated to boiling temperature (~56°C) and refluxed approximately for 30 min. The hot solution was filtered and the filtrate left at ambient conditions to slowly evaporate the solvent. Colorless rectangular thin-plate crystals appeared after 3 days [17, 20, 21].

Nifedipine Polymorphic Form α

We dissolved 190 mg of nifedipine powder in a mixture of 6 ml of acetone and 4 ml of methanol, heated to boiling temperature (~56°C) and refluxed for 15 min. The hot solution was filtered and the filtrate left at ambient conditions to slowly evaporate the solvent. Yellow rectangular thin-plate crystals appeared after a few hours [22].

Olanzapine Polymorphic Form I

We dissolved 250 mg of olanzapine in 20 ml of ethyl acetate. The mixture was slowly heated to boiling temperature (~77°C) and refluxed for approximately 15 min. The hot solution was filtered and the filtrate left at ambient conditions to slowly evaporate the solvent. Yellow prismatic crystals appeared after 1 day [23].

METHODS

Identification of Polymorphic Forms

The structures of APIs' single crystals were examined by single-crystal X-ray diffraction to confirm polymorphic forms. For crystalline powders (used for bulk study), structures were confirmed with differential scanning calorimetry (DSC) and Fourier transform infrared spectroscopy (FTIR).

Single-Crystal X-ray Diffraction (SCXD)

All crystalline samples studied were carefully examined under a stereomicroscope. Defect-free single crystals were chosen. A limited set of diffraction data was collected for each selected crystal on an Agilent SuperNova diffractometer at room temperature to identify its polymorphic form. The face indexing on each individual crystal was performed prior to nanoindentation studies using CrysAlis PRO software (CrysAlis PRO. Agilent Technologies UK Ltd., Yarnton, UK).

Thermal Analysis

Differential Scanning Calorimetry (DSC). Thermograms were recorded by DSC, Mettler Toledo instrument (Columbus, OH, USA). Samples (~5 mg) were placed in covered, pierced aluminium pans under an N_2 atmosphere (flow rate 50 ml/min). The heating rate for famotidine, nifedipine, and olanzapine was 10°C/min and the heating rate for piroxicam was 5°C/min. A temperature interval from 25 to 190°C was applied to the famotidine and nifedipine, and an interval from 25 to 210°C was used for olanzapine and piroxicam polymorphic forms.

Fourier Transform Infrared Spectroscopy (FTIR)

FTIR spectra were obtained with a Thermo Nicolet Nexus instrument (Nicolet Instrument Co., USA) with an ATR DuraSamplIR attachment (Smith Detection Group). Data were acquired using OMNIC software (version 5.2, Nicolet Instrument Co.). MID spectra were recorded between 4,000 and 600 cm^{-1} with an instrument resolution of 8 cm^{-1}. Each individual spectrum was an average of 32 scans.

DETERMINATION OF MECHANICAL PROPERTIES OF POLYMORPHS

Nanoindenter

Sample Preparation. The oriented crystals were fixed to the surface of the cover glass with fast-hardening epoxy resin (UHU plus, immediately fixed adhesives, GmbH, Buhl, Germany) and glued to the metallic sample support equipped with the nanoindenter. Defect-free crystals of each material investigated were chosen for nanoindentation studies. The number of indents on a specific face of a crystal varied from three to 40, which depended on the crystal size and its surface quality (absence of surface imperfections).

Nanoindentation Measurement

In the individual experiments, nanoindentation was performed at room temperature using an Agilent G200 Nanoindenter (Agilent, Santa Clara, CA, USA). A three-sided pyramidal Berkovich indenter was utilized to determine the mechanical properties of the single crystals studied. Thermal drifts were ensured to be consistently low (typically <0.05 nm/s). Moreover, nanoindentation experiments were conducted under continuous stiffness measurement (CSM) mode. Young's modulus (E) and indentation hardness (H) were obtained as a function of the indentation depth (max. 700 nm). This was attained by superimposing a 2 nm sinusoidal displacement at 45 Hz onto the primary loading signal, while tracking the system response via a frequency-specific amplifier. The loading and unloading strain rate targets were set at 0.05 s^{-1}. At the maximum displacement of 700 nm, the indenter was held for 15 s prior to unloading in order to minimize the creep effect. According to the dynamic CSM mode, E and H are determined as a function of the sample penetration depth (h). The calculation principle is based on a simple harmonic oscillator subjected to a force oscillation:

$$K = \left(S^{-1} + K_f^{-1}\right) + K_s K = \left(S^{-1} + K_f^{-1}\right) + K_s \qquad (1)$$

where K is equivalent stiffness (including the stiffness of the contact S), K_f is load frame stiffness, and K_s is the stiffness of the

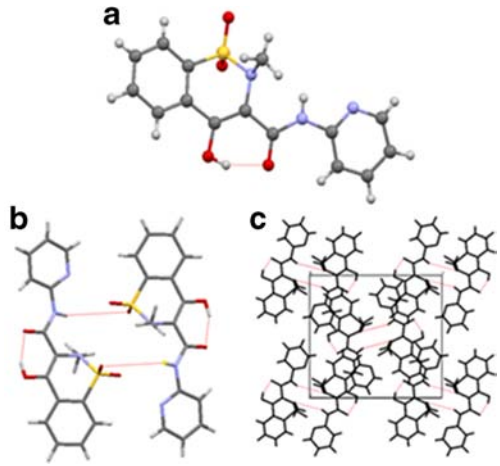

Fig. 1 Molecular structure of piroxicam I. The intramolecular hydrogen bond is shown as a red dotted line (**a**). Centrosymmetric dimer of piroxicam molecules formed by two hydrogen bonds (**b**) and the orientation of the dimers in the crystal lattice (**c**).

support springs. Furthermore, stiffness (S) of the sample and damping of the contact ($D_s\omega$) are given by:

$$S = \left(\frac{1}{\frac{F_0}{z_0} cos\varphi - (Ks - m\omega^2)} - \frac{1}{K_f} \right)^{-1} \quad (2)$$

$$D_s\omega = \frac{F_0}{z_0} sin\varphi - D_i \quad (3)$$

In the CSM mode, the excitation frequency (ω) is a set value. During the experiments, we measured the displacement amplitude (z_0), phase angle (φ), and excitation amplitude (F_0). The damping factor of the indenter head (D_i), K_s, and parameter m are machine factors determined by analyzing the system dynamic response when the indenter is hanging free. The elastic modulus of the test sample E is determined from the reduced

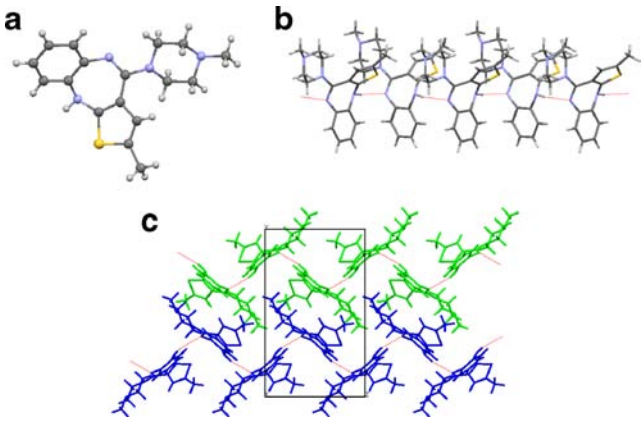

Fig. 2 The molecular structure of olanzapine (**a**) and the formation of infinite chains through hydrogen bonds (**b**). Packing diagram of olanzapine I viewed along the a-axis, showing the orientation of two zigzag chains (**c**).

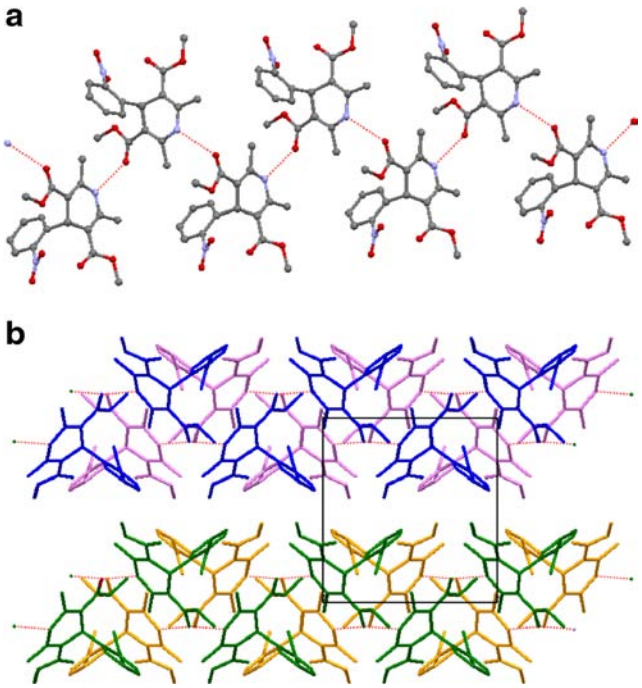

Fig. 3 Nifedipine molecules connected through hydrogen bonds into infinite chains propagated along the b-axis (**a**). The packing diagram of nifedipine viewed along the c-axis. Four infinite chains are presented, colored green, orange, blue, and violet (**b**)

modulus (E_r), given by:

$$E_r = \frac{\sqrt{\pi}}{2\beta} \frac{S}{\sqrt{A_c}} \quad (4)$$

where A_c is the projected contact area and β is a constant that depends on the indenter's geometry ($\beta = 1.034$ for the Berkovich tip).

Referring to Oliver and Pharr's theory [4, 24], E can be extracted from the following equation:

$$\frac{1}{E_r} = \frac{1-v_s^2}{E_s} + \frac{1-v_i^2}{E_i} \quad (5)$$

where E_i and v_i represent the elastic modulus and Poisson's ratio of the indenter (for the diamond tip: $E_i = 1{,}141$ GPa and $v_i = 0.07$), and E_s represents the elastic modulus of the sample.

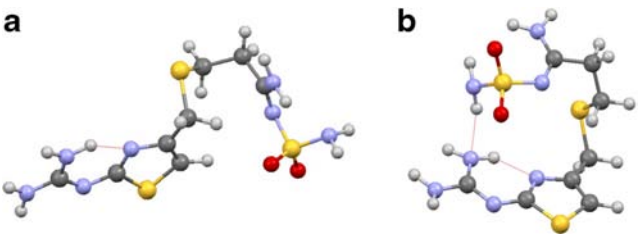

Fig. 4 Molecular structures of the two polymorphs of famotidine: famotidine A (**a**) and famotidine B (**b**). Intramolecular hydrogen bonds are shown as red dotted lines.

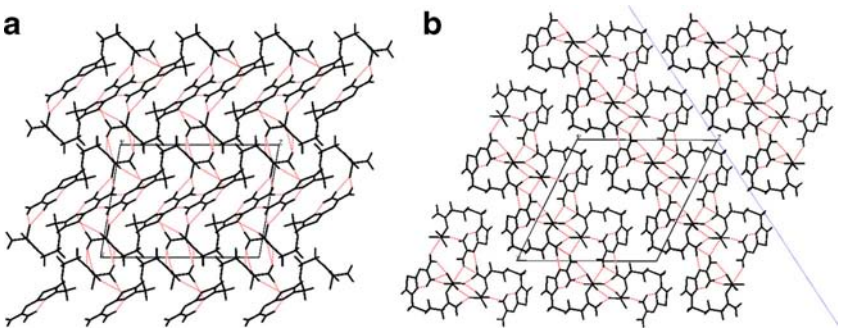

Fig. 5 A packing diagram of famotidine A (**a**) and famotidine B (**b**), viewed along the b-axis. Hydrogen bonds are shown as red dotted lines. The slip plane (−101) in form B is presented as a red line.

The indentation hardness H is calculated as the ratio between the applied load (P) and projected contact area (A_c):

$$H = \frac{P}{A_c} \tag{6}$$

The projected contact area is calculated by evaluating an empirically determined area function of the contact depth, h_c:

$$A = f(h_c) \tag{7}$$

$$h_c = h_{max} - \varepsilon\left(\frac{P_{max}}{S}\right)$$

where h_{max} is the maximum penetration depth, ε is a geometric constant of the Berkovich indenter, and (P/S) expresses the extent of elastic recovery.

Assessment of the Bulk Mechanical Properties

To eliminate the influence of particle size on bulk mechanical properties, the materials studied were first ground in a mortar to comparable particle sizes. This was confirmed with laser diffractometry (Mastersizer S, Mavern Instruments, Malvern, UK) by measuring the median (d_{50}) and average (D [3,4]) particle size, as well as width of distribution (SPAN). Powders were dispersed in water and pumped using a small volume dispersion unit. When applicable, a few drops of 1% SDS solution were added to improve the wetting.

Bulk mechanical properties were determined by compressing the powders with a factory-instrumented single-punch tableting press (Kilian SP300, IMA, Cologne, Germany) with round flat-faced punches (d=12 mm) without a beveled edge. The compression force was measured by full Wheatstone bridge strain gauges on the lower and upper punches, coupled with a linear displacement transducer mounted on the upper punch. Tablets of each sample were compressed at pressures ranging from 30 to 180 MPa at a tableting rate of 25 tbl/min. Prior to compaction, the punches were lubricated with 1% suspension of Mg-stearate in isopropanol. Tablet mass was determined using a precise analytical balance (Sartorius 1,773, Göttingen, Germany). At each compression pressure, 10 tablets were evaluated 24 h after compression and their dimensions were acquired. These dimensions were measured with an outside micrometer (series 103–137; 0–25 mm; 0.01 mm; Mitutoyo, Kawasaki, Japan).

The elastic relaxation index (ER) was determined using the following Eq. 8 [25]:

$$ER = \frac{H_1 - H_0}{H_0}[\%] \tag{8}$$

where H_0 is tablet thickness under maximum pressure inside the die and H_1 24 h after compression outside the die. For the single vs. bulk study, data obtained at 130 MPa were used for the ER index. The increase in tablet thickness corresponds to the elasticity of the material exerted at the bulk level.

Table I Summary of Crystal Data of the Compounds Examined

	Piroxicam I	Famotidine A	Famotidine B	Nifedipine α	Olanzapine I
Crystal system	monoclinic	monoclinic	monoclinic	monoclinic	monoclinic
Space group	$P2_1/c$	$P2_1/c$	$P2_1/n$	$P2_1/c$	$P2_1/c$
a (Å)	7.127 (2)	11.9115 (3)	16.980 (2)	10.923 (5)	10.328 (3)
b (Å)	15.136 (7)	7.1876 (2)	5.285 (1)	10.326 (6)	14.524 (3)
c (Å)	13.949 (6)	16.6236 (4)	17.639 (2)	14.814 (7)	10.500 (3)
α	90.00	90.0	90.00	90.00	90.00
β	97.35 (4)	100.045 (1)	116.416 (1)	92.70 (6)	100.606 (14)
γ	90.00	90.00	90.00	90.00	90.00
References	27	28	30	26	29

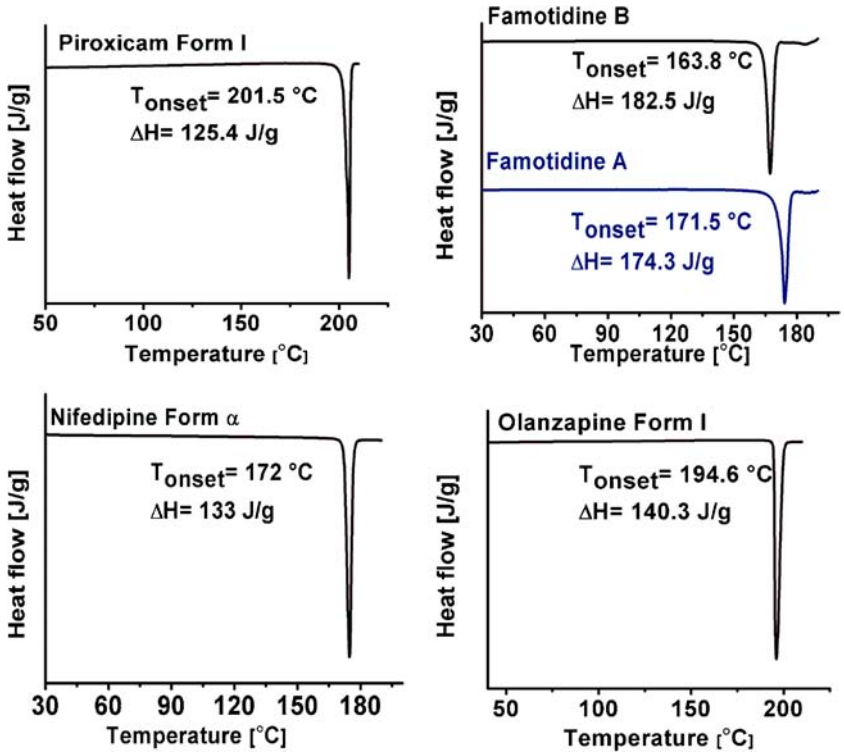

Fig. 6 DSC thermograms of polymorphic forms investigated.

RESULTS AND DISCUSSION

Analysis of Molecular Packing Pattern With Respect to Crystal Orientation

Piroxicam

The molecular structure of confirmed form I is presented in Fig. 1a. Form I with the highest melting point is the most stable one, and it is used in pharmaceutical products [8]. The molecular structure is stabilized by a strong intramolecular hydrogen bond between a hydroxyl group and a carbonyl oxygen atom. The ring system, including the hydroxyl and carbonyl groups, is close to planar, with the methyl group and one of the two oxygen atoms of the SO_2 group protruding from the plane on different sides.

Within the crystal, molecules are connected through an intermolecular hydrogen bond between the amide group as a donor and oxygen atom of the sulfoxide group as acceptor to form centrosymmetric dimers, presented in Fig. 1b. Such dimers are packed to form a herringbone type of arrangement and, despite the lack of other intermolecular hydrogen bonds, the structure can be envisioned as "mechanically interlocked" (Fig. 1c).

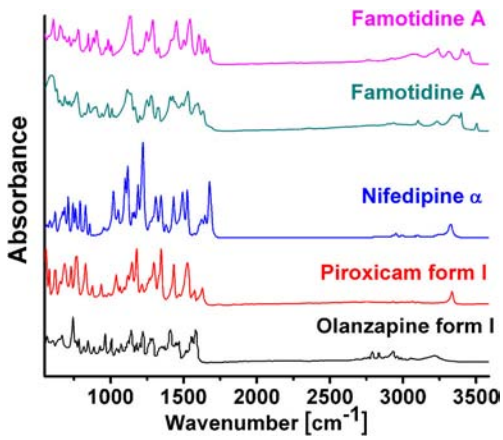

Fig. 7 FTIR spectra of polymorphic forms investigated.

Olanzapine

The molecular structure of olanzapine form I is shown in Fig. 2. As expected, no intramolecular hydrogen bonds are observed. However, an intermolecular hydrogen bond of the

Table 2 Assignments for the Infrared Absorption Bands of Piroxicam form I

Frequencies [cm^{-1}]	Assignments
3,344	Stretching of OH group
1,625	Stretching of amine carbonyl group
1,532	Stretching of second amine band
1,439	Stretching of asymmetric methyl group
1,350	Stretching of symmetric methyl group
1,142	Stretching of SO_2-N group
765	Stretching of ortho-disubstituted phenyl group
682	C-S stretching

Table 3 Assignments for the Infrared Absorption Bands of Nifedipine form α

Frequencies [cm^{-1}]	Assignments
3,330	Stretching of the N-H group
2,951	Stretching of the aromatic CH_3 group
1,697	Stretching of the ester carbonyl band
1,490–1,532	Stretching of the aromatic C-C band
1,305	Stretching of the NO_2 group
1,230	Ether absorption band of C5

type N-H…N connects the molecules into infinite zigzag chains. Such chains are propagated along the c-axis and are packed together densely, as shown in Fig. 2b. Again, the system can be described as mechanically interlocked (Fig. 2c).

Nifedipine

The crystals of nifedipine investigated belong to a monoclinic polymorphic form structurally described by Triggle et al. [26]. No typical intramolecular hydrogen bond was observed. The molecules are connected by hydrogen bonds between an endocyclic N atom as a donor and carbonyl oxygen of the neighboring molecule as an acceptor to form infinite zigzag chains (Fig. 3a). The chains are packed in the crystal as shown in Fig. 3b.

Famotidine

The structures of the famotidine polymorphs show markedly different molecular conformations (Fig. 4). Famotidine A possesses one intramolecular hydrogen bond between the guanidine amino group as a donor and the endocyclic thiazole nitrogen atom as an acceptor. The molecular structure of famotidine B is stabilized by two intramolecular hydrogen bonds: i) one being of the same type as observed in form A and ii) an additional contact between sulfamoyl NH_2 group as a donor to the guanidine N atom (Fig. 4b). This additional interaction forces the molecule to exist in a kind of "folded" conformation. Consequences of different molecular structures are reflected in different packing schemes.

Molecules of form A are connected by hydrogen bonds to form a densely packed three-dimensional network (Fig. 5). The molecules are highly cross-linked through H-bonds and the nature of extensive intermolecular interactions can be considered as nearly the same in all directions. Famotidine B shows a distinctly different packing arrangement. Molecules are connected through hydrogen bonds to form layers parallel to (−101). These layers present a slip system together with the associated slip direction <101>. The shape of the crystals of form B was anisotropic, and so the indentation measurements were performed in such a way that the loading axis was always normal to the major face (−101), which was equivalent in all the crystals examined.

All structures have already been reported in the literature and their crystallographic data are presented in Table 1.

Solid State Characterization of API Polymorphic Forms

Thermal Analysis of Polymorphs. DSC thermograms of the polymorphic forms investigated, with measured onset temperatures and melting enthalpies, are presented in Fig. 6. Form I of piroxicam was successfully prepared by recrystallization

Table 4 Assignments for the Infrared Absorption Bands of Famotidine

Frequencies [cm^{-1}]		Assignments
Form A	Form B	
3,456 (strong)	3,502 (strong)	asymmetric stretching of NH_2 groups from guanidine and sulfamoyl group
3,409 (strong)	3,409 (strong)	symmetric stretching of NH_2 groups from guanidine and sulfamoyl group
3,312 (strong)	3,352 (strong)	stretching of NH_2 (sulfo), stretching of C-H (thiazole), asymmetric stretching of CH_2, symmetric stretching of CH_2
3,246 (strong)	3,237 (strong)	stretching of NH_2 (sulfo), stretching of C-H (thiazole), asymmetric stretching of CH_2, symmetric stretching of CH_2
3,065 (strong)	3,112 (strong)	stretching of NH_2 (sulfo), stretching of C-H (thiazole), asymmetric stretching of CH_2, symmetric stretching of CH_2
1,667 (strong)	1,634 (strong)	stretching of C = N (guanidine)
1,602 (strong)	1,597 (strong)	deformational bending of (NH2) in guanidine, stretching of (N–C = N)
1,546 (strong)	1,523 (strong)	deformational bending of (NH2) sulfo + δ (thiazole), deformation of CH_2
1,499–1,416 (medium)	1,486–1,402 (medium)	Ring stretching modes
1,286 (strong)	1,262 (strong)	Deformational bending of thiazole + out of plain deformation of (CH_2–S), deformational bending of (C thioether–thiazole), stretching of (C–C)
1,197 (strong)	1,174 (strong)	stretching of (SO_2) and symmetric stretching of (SO_2) modes
900 (strong)	905 (strong)	stretching of the N-S band

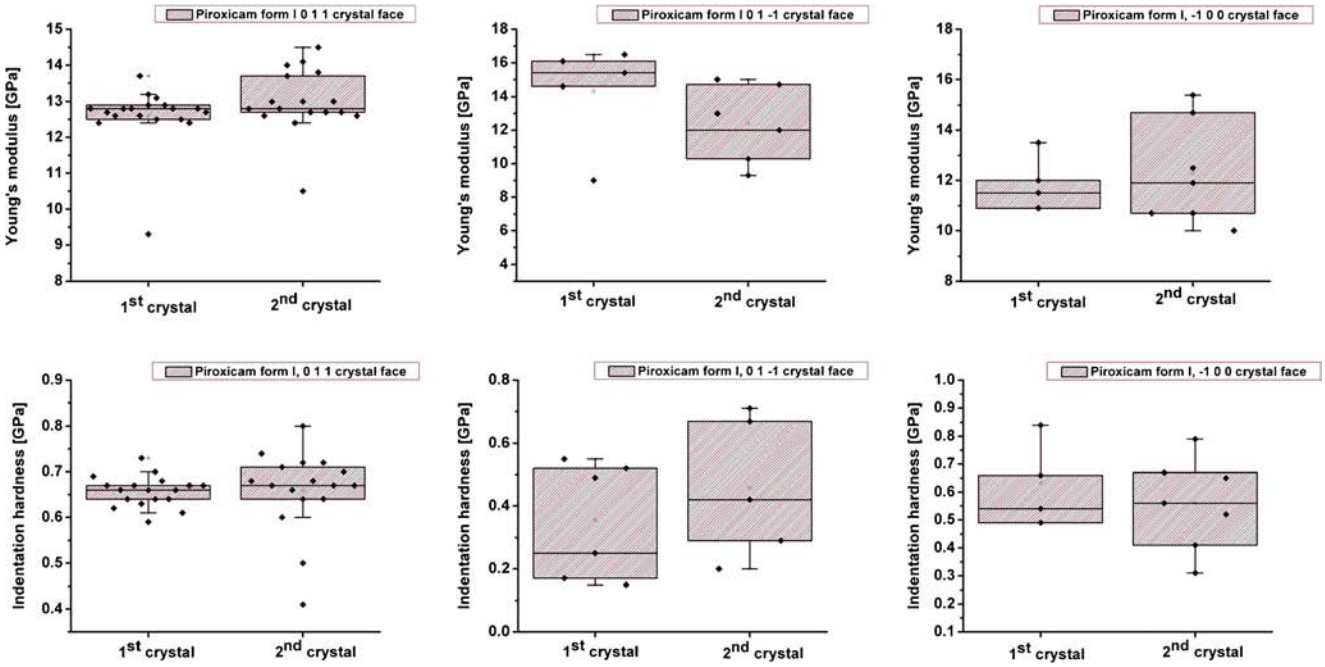

Fig. 8 Box-plot of mechanical properties (Young's modulus and indentation hardness) of single crystals of piroxicam form I with respect to crystal face orientation.

from benzyl alcohol, as previously stated in the literature. The endothermic peak at 201.5°C corresponds to form I [18].

The onset temperature of about 194°C is related to the melting point of olanzapine form I, prepared by recrystallization from ethyl acetate [30].

The thermodynamically stable form α of nifedipine, isolated from the mixture of acetone and methanol, demonstrates a single sharp endothermic peak at 172°C, corresponding to its melting point [23].

The DSC curve of famotidine form B, obtained by crystallization from a methanol/acetone mixture, exhibits a single sharp endothermic peak at 163.8°C, representing its melting point. Form A was successfully prepared by recrystallization from acetonitrile, as reported in the literature. The presence of an endothermic peak at 171.5°C was found for famotidine form A [22].

All DSC data obtained for the polymorphic forms investigated are consistent with the previously reported results from other studies [18, 22, 23, 30].

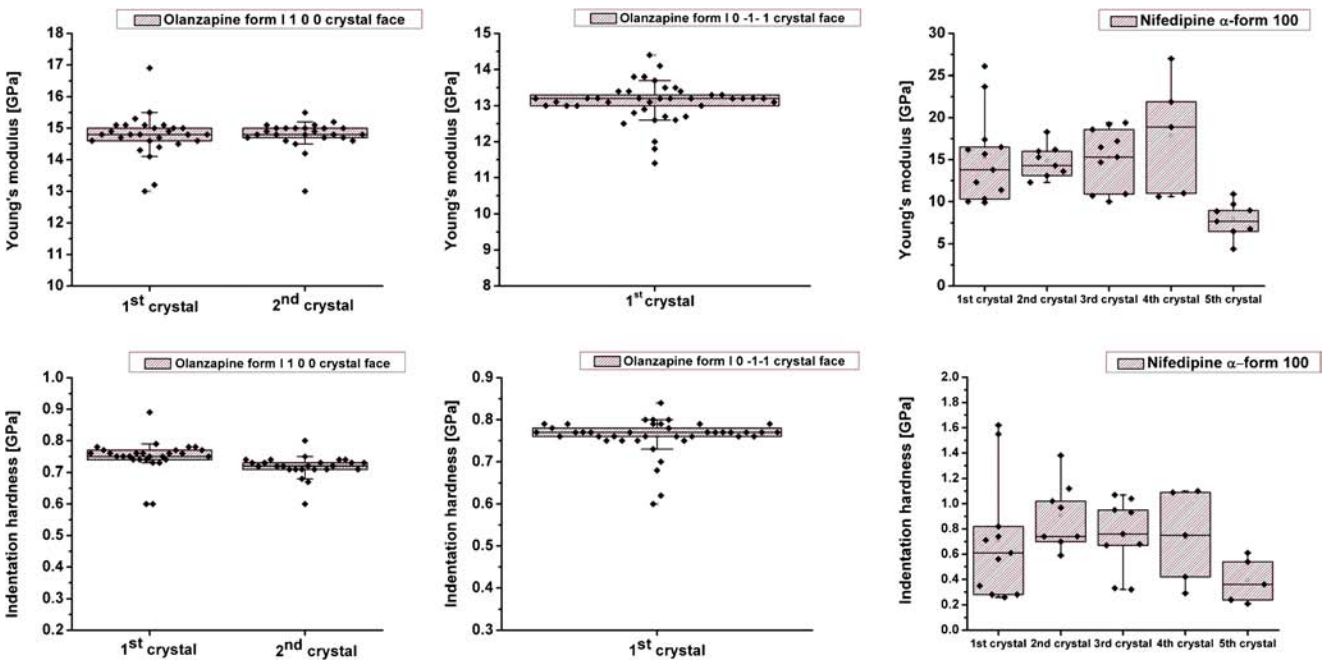

Fig. 9 Box-plot of mechanical properties (Young's modulus and indentation hardness) of single crystals of nifedipine form α and olanzapine form I with respect to crystal face orientation.

Spectroscopic Identification of Polymorphic Forms

The IR spectra of the polymorphic forms investigated are shown in Fig. 7.

The FTIR spectra of piroxicam show a band at 3,344 cm^{-1} (Fig. 7), which indicates that the drug is in the cubic polymorphic form. Vibrational assignments characteristic for piroxicam form I are represented in Table 2 and are in good agreement with the literature data [18].

The olanzapine molecule consists of piperazine, thiophene, and azepine moieties and possesses complex vibrational spectra. The following bands are attributed to the stretching of different group vibrations and are specific for olanzapine form I: 3,224 cm^{-1} stretching of the amino group, 2,945 cm^{-1} stretching of the C-H group, stretching of C=C and C=N belonging to the benzene and thiophene rings, 1,220 cm^{-1} N-H stretching, 1,086 cm^{-1} OH bending, 1,016 cm^{-1} deformation of the piperazinyl group coupled with methyl, 960 cm^{-1} vibration of azepine and thiophene moieties, and 751 cm^{-1} stretching of the C-S group.

According to the IR spectra, the α-form of nifedipine can be identified. Characteristic vibrational bands of α-nifedipine are represented in Table 3.

The famotidine molecule consists of guanidine, thiazole, thioether, and sulfamoyl parts. Vibrational assignments characteristic for both polymorphic forms of famotidine investigated are presented in Table 4.

In the case of famotidine A and B, characteristic absorption bands at 3,456 and 3,502 cm^{-1} were observed, respectively, and correspond to asymmetric stretching of the NH_2 group from guanidine and sulfamoyl moieties. The detected absorption bands were used as fingerprint markers for differentiation between form A and B of famotidine and were consistent with the literature data [30, 31].

Mechanical Properties of Pharmaceutical Crystals

The indentation depth (max. 700 nm) chosen in this nanoindentation study was related to the application of small loads for testing mechanical properties of single crystals. Such an approach increased the measurement resolution and decreased the extensive crack formation as well as the amount of pile-up, which generally led to a reduction of the Young's modulus and indentation hardness.

In most cases, two crystals were oriented and mechanically mapped, with the exception of nifedipine form α, from which five single crystals were tested. The main reason for this was the cracking of the crystal's surface due to its photosensitivity, which influenced large variability of the results (crystals are exposed to microscopic light during the initial setup at the nanoindenter).

For piroxicam form I, comparable values of *E* and *H* were determined with respect to mapped crystal faces (0–1 − 1, 0 1

Table 5 Mechanical Properties of Crystals Investigated with Regard to Crystal Face (*E* = Young's modulus; *H* = indentation hardness). All results are represented as median values ± interquartile ranges

Sample	Crystal face															
	−1 0 0		1 0 0		0 −1 −1		0 1 1		−1 0 1		0 1 −1		0 0 −1			
	E GPa	H	E	H	E	H	E	H	E	H	E	H	E	H		
Piroxicam form I	11.9 ± 2.8	0.56 ± 0.18					12.8 ± 0.04	0.67 ± 0.04			14.6 ± 0.3	0.42 ± 0.02				
Famotidine form A	22.6 ± 2.0	1.58 ± 0.4											20.1 ± 1.2	1.33 ± 0.16		
Famotidine form B									19.5 ± 0.4	0.84 ± 0.16						
Nifedipine α- form			13.8 ± 6.9	0.71 ± 0.61												
Olanzapine form I			14.8 ± 0.4	0.74 ± 0.04	13.2 ± 0.3	0.72 ± 0.02										

1, −1 0 0; Fig. 8). The reason for such results can be found in the "mechanically interlocked structure" in all crystal orientations. The larger variation of the results for crystal faces 0–1 − 1 and −1 0 0 is related to the smaller number of indentations performed on these surfaces (Fig. 8).

The structure of olanzapine form I can be described as mechanically interlocked because the intermolecular hydrogen bond of the type N-H…N connects the molecules into infinite zigzag chains. As a result, significant differences of *E* and *H* with respect to the oriented crystal face were not determined (Fig. 9). Plastic deformation is limited because slip between interlocked layers is restricted. As a consequence, olanzapine crystals demonstrated a significant extent of elastic relaxation (Fig. 11).

Nifedipine form α single crystals were oriented at just one crystal face, 1 0 0. Nifedipine molecules are connected though hydrogen bonds into infinite chains propagated along the b-axis. The layers are deeply interdigitated, which makes slippage more difficult. The crystals demonstrated the largest extent of elastic relaxation (Fig. 11). The coefficient of variation for *E* and *H* was found to be large, which is related to the cracking of the surface (increasing the surface roughness), induced by light. Modest reproducibility of the results was especially evident for nifedipine hardness values (Fig. 9).

According to the values of *H*, the least plastic properties were determined for famotidine form A, whereas all other crystals have comparable values of *H* without regard to crystal orientation (face) (Table 5, Figs. 8, 9 and 10). The clear dependence of mechanical properties on the molecular packing (polymorphism) was noticed for famotidine (Table 5). The polymorphic forms of famotidine investigated differ in their arrangement of intramolecular hydrogen bonds.

For form A, a densely packed three-dimensional network is specific. The molecules are highly cross-linked through H-bonds, due to which the structure is interlocked. The better packing and three dimensional nature of the hydrogen bond network is manifested in higher *E* and *H* in comparison to famotidine B (Fig. 10). This is additionally confirmed by the higher true density of famotidine A (data not shown). Because the structure is interdigitated in all directions, significant differences in mechanical properties at the crystal faces investigated were not established. It is likely that the intermolecular nature of bonds rather than intramolecular forces strained conformation and reduced flexibility, which resulted in lesser plasticity and higher stiffness of famotidine form A. Such observation was also confirmed at the bulk level with lower elastic relaxation of famotidine A in comparison to form B (Fig. 11).

On the other hand, the anisotropic properties of famotidine form B are related to parallel organization of layers connected with hydrogen bonds, which are parallel to −1 0 1. In this case, the nanoindentation was performed in a direction normal to the slip planes. Such a manner of material exposure to deformational forces neither induced the massive cracking of the crystal surface nor pop-ins. Lower indentation hardness for this polymorphic form can be explained with higher density in one direction, which decreased the attachment energy of stacking layers and stiffness but improved its plasticity. The presence of slip planes improved mechanical

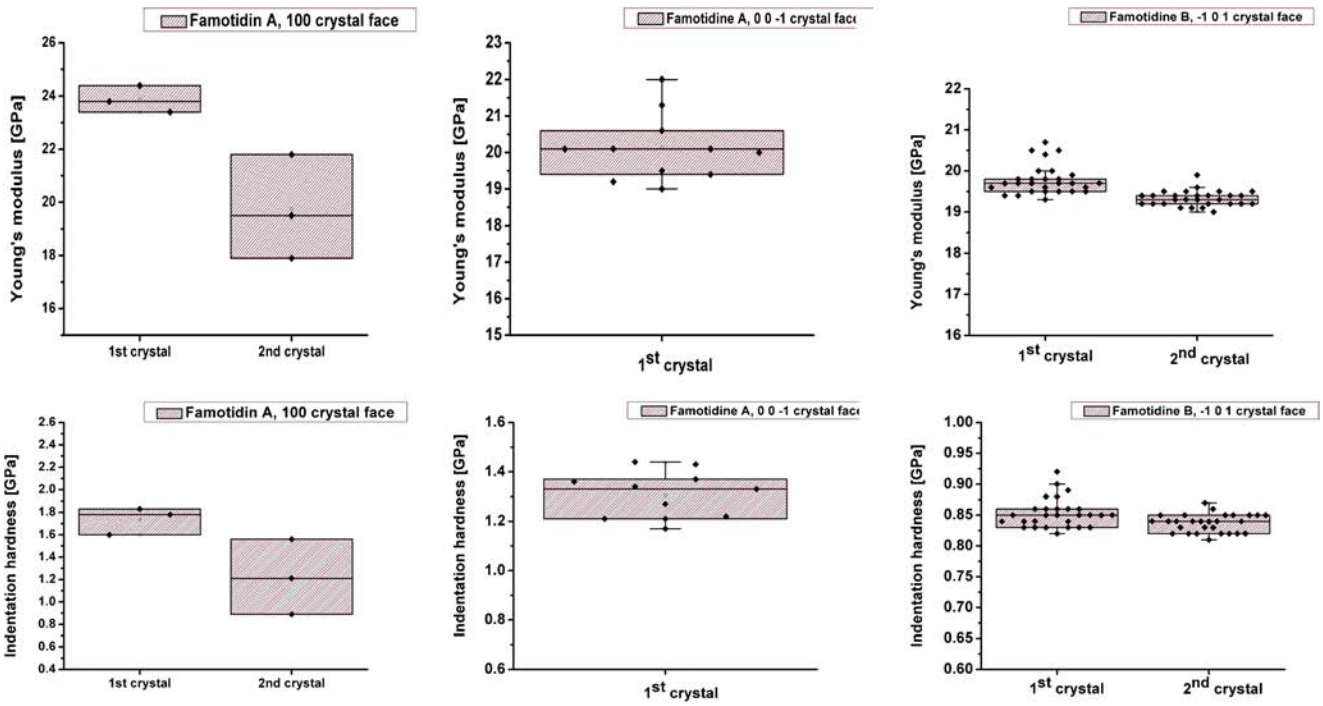

Fig. 10 Box-plot of mechanical properties (Young's modulus and indentation hardness) of single crystals of famotidine form A and B with respect to crystal face orientation.

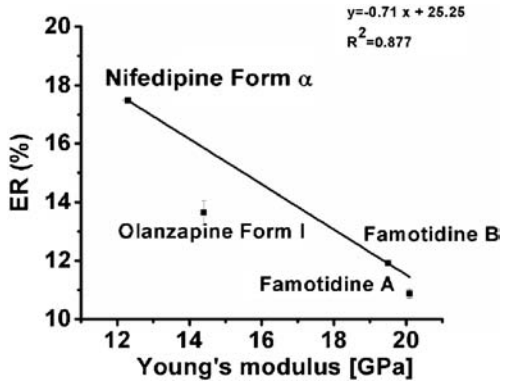

Fig. 11 Correlation between elastic relaxation of tablets (*ER*) and Young's modulus (*E*) of crystals investigated.

properties by allowing slip of the layer over adjacent ones, resulting in higher plasticity at the single-particle level. This was confirmed at the bulk level with lower yield pressure of famotidine A in comparison to B (data not shown). A summary of the results for the mechanical properties of the APIs investigated is presented in Table 5. Generally, good reproducibility of the results was observed across the single crystals investigated. This implies that nanoindentation can be used for reliable characterization of pharmaceutical materials whether as a single sample or over a number of batches. The technique is rapid and not material-intensive, allowing quick determination of crystals' mechanical properties.

No discrepancies were determined between the packing of molecules at the crystal faces tested and the elastic and plastic parameters of the polymorphic forms investigated. In order to evaluate the mechanical behavior of the materials investigated, yield pressure (P_y) and its ratios with E and H and were calculated according to Eq. 9 [32]:

$$\frac{H}{P_y} = 0.07 + 0.6\ ln\ \frac{E}{Py} \tag{9}$$

P_y generally gives an indication of the elastic limit and flow stress of materials. Categorization of the material is presented in Table 6. According to the ratios of H/P_y, materials can be classified as very elastic if H/P_y is 1.5–2.0; brittle if H/P_y is 2.0–2.2, and plastic if $H/P_y \geq 3.0$ [32].

For all materials investigated, a brittle nature can be confirmed. According to the ratio between E/P_y, the elastic component of deformation is more emphasized in the case of piroxicam form I, nifedipine olanzapine, and famotidine B, which is confirmed at the bulk level with a larger ER index.

Single-Crystal Versus Bulk Mechanical Properties

Poor compressibility of a powder is generally related to the lack of a material's plasticity during tableting, which might be accompanied by high elastic recovery in the decompression phase. The final tablet properties are generally considered as equilibrium of the stored elastic energy as the driving force for the tablet expansion, and particle bonding as a counteracting force [33]. Extensive elastic relaxation as a consequence of a small number of weak bonds at the contacting surfaces at the atomic distance formed during compression leads to poor tablet strengths and, in extreme cases, to lamination.

The tablets' stress relaxation is quantitatively expressed as an index of elastic relaxation (*ER*) and represents the relative increase of tablet thickness in percent after being ejected from the die. This parameter is commonly used to determine a material's elasticity on the bulk scale [33–35]. As a comparable parameter of elasticity of single crystals, median values of overall E obtained for crystals without regard to crystal face were used for the correlation study.

The correlation between the bulk parameter *ER* and the previously mentioned single-particle elasticity parameter is shown in Fig. 11. Our results show that a tablet's elastic relaxation largely depends on the intrinsic elastic attribute of the materials, as evident from the positive correlation between ER and E ($R^2 = 0.81$). According to these results, the nanoindentation measurement for the single crystals can even be used as a tool for predicting elastic behavior during compression for APIs [34, 35]. In this case, only crystal structures (molecular packaging and bond strength) have been taken into consideration as responsible for mechanical behavior at the bulk level. There are numerous approaches for improvement of compression properties of crystalline materials with no alteration of their crystal structures such as formation of core-shell material [36] or by modification of process for powder preparation with quench-cooling [37].

CONCLUSION

The mechanical properties of the APIs' polymorphic forms investigated were successfully determined at a single-crystal level by using a nanoindenter. This technique provided reproducible data using only a small number of single crystals.

Table 6 Yield Pressure (P_y) and Ratios for E/P_y and H/P_y for Materials Investigated

Parameters	Piroxicam form I	Famotidine A	Famotidine B	Nifedipine α	Olanzapine form I
P_y [MPa]	221 ± 68	720 ± 37	335	300	310 ± 0.5
E/P_y	59.3	29.6	60.4	60.4	45.2
H/P_y	2.5	2.1	2.5	2.5	2.4
Categorization	Brittle/elastic	Brittle	Brittle/elastic	Brittle/elastic	Brittle/elastic

Mechanical properties such as Young's modulus and indentation hardness were consistent with the molecular packing of the polymorphic forms investigated with respect to crystal orientation. For mechanically interlocked structures, characteristic of most polymorphic forms, response of single crystals to indentation was isotropic. The predictive value of nanoindentation was demonstrated by good correlation between bulk elastic properties (elastic relaxation index of compressed tablets) and Young's modulus at the single-crystal level.

The results confirm the idea that the intrinsic mechanical properties of active ingredients (Young's modulus) largely control and anticipate their behavior during tableting. Young's modulus and indentation hardness might therefore represent very valuable information in preformulation studies for evaluating materials' mechanical attributes, which are important for technological processes in which materials are exposed to deformation.

REFERENCES

1. Chong Tan J, Furman JD, Cheetham AK. Relating mechanical properties and chemical bonding in an inorganic–organic framework material: a single crystal nanoindentation study. J Am Chem Soc. 2009;131:14252–4.
2. Shariare MS, Leusen FJ, Matas M, York P, Anwar J. Prediction of the mechanical behaviour of crystalline solids. Pharm Res. 2012;29: 319–31.
3. Hudson RJ, Zioupos P, Gill PP. Investigating the mechanical properties of RDX crystals using nanoindentation. Propellants Explos Pyrotech. 2012;37:191–7.
4. Oliver WC, Pharr GM. An improved technique for determining hardness and elastic-modulus using load and displacement sensing indentation experiments. J Mater Res. 1992;7:1564–83.
5. Pharr GM. Measurement of mechanical properties by ultra-low load indentation. Mat Sci Eng A-Struct. 1998;253:151–9.
6. Jing Y, Zhang Y, Blendell J, Koslowski M, Carvajal MT. Nanoindentation method to study slip planes in molecular crystals in a systematic manner. Cryst Growth Des. 2011;11:5260–7.
7. Varughese S, Kiran MSRN, Solanko KA, Bond AD, Ramamury U, Desiraju GR. Interaction anisotropy and shear instability of aspirin polymorphs established by nanoindentation. Chem Sci. 2011;2(11): 2236–42.
8. Kiran MSRN, Varughese S, Reddy CM, Ramamurty U, Desiraju GR. Mechanical anisotropy in crystalline saccharine: Nanoindentation studies. Cryst Growth Des. 2010;10:4650–5.
9. Meier M, John E, Wieckhusen D, Wirth W, Peukert W. Influence of mechanical properties of impact fracture: Prediction of the milling behavior of pharmaceutical powders by nanoindentation. Powder Technol. 2009;188:301–131.
10. Reddy CM, Basavoju S, Desiraju GR. Sorting of polymorphs based on mechanical properties. Trimorphs of 6-chloro-2,4-dinitroaniline. Chem Comm. 2005;19:2439–41.
11. Zugner S, Marquardt K, Zimmermann I. Influence of nanomechanical crystal properties on the comminution process of particulate solids in spiral jet mills. Eur J Pharm Biopharm. 2006;62:194–201.
12. Feng Y, Grant DJW. Influence of crystal structure on the compaction properties of n-alkyl 4-hydroxybenzoate esters (parabens). Pharm Res. 2006;23(7):1608–16.
13. Shakhtshneider TP, Boldyreva EV, Vasilchenko MA, Ahsbahs H, Uchtmann H. Anisotropy of crystal structure distortion in organic molecular crystals of drugs induced by hydrostatc compression. J Struct Chem+. 1999;40(6):892–8.
14. Boldyreva EV, Shakhtshneider TP, Vasilchenko MA, Ahsbahs H, Uchtmann H. Anisotropic crystal structure distortion of the monoclinic polymorph of acetaminophen at high hydrostatic pressure. Acta Crystalogr B. 2000;B56:299–309.
15. Boldyreva EV. Anisotropic compression. What can it teach us about intermolecular interactions? In: High-Pressure Crystallography. From Novel Experimental Approaches to Applications in Cutting-Edge Technologies (Eds. E. Boldyreva, P. Dera), Springer: Dordrecht, 2010, 147–159.
16. Boldyreva EV. High-pressure studies of pharmaceuticals and biomimetics. Fundamentals and applications. A general introduction. In: High-Pressure Crystallography. From Novel Experimental Approaches to Applications in Cutting-Edge Technologies (Eds. E. Boldyreva, P. Dera), Springer: Dordrecht, 2010, p.533-543.
17. Hegedus B. Morphologically homogenous forms of famotidine and processes for their preparation. EU Patent. 2001;0256747:1–10.
18. Vrečer F, Vrbinc M, Meden A. Characterization of piroxicam crystal modifications. Int J Pharm. 2003;256:3–15.
19. Lu J, Wang XJ, Yang X, Ching CB. Polymorphism and crystallization of famotidine. Cryst Growth Des. 2007;7(9):1590–8.
20. An JH, Kim JM, Chang SM, Kim WS. Application of ionic liquid to polymorphic design of pharmaceutical ingredients. Cryst Growth Des. 2010;10:3044–50.
21. Hassan MA, Salem MS, Seeliman MS, Najib NM. Characterization of famotidine polymorphic forms. Int J Pharm. 1997;149:227–32.
22. Caira MR, Robbertse Y, Bergh JJ, Song M, De Villiers MM. Structural characterization, physicochemical properties, and thermal stability of three crystal forms of nifedipine. J Pharm Sci. 2003;92: 2519–33.
23. Reutzel-Edens SM, Bush JK, Magee PA, Stephenson GA, Byrn SR. Anhydrates and hydrates of olanzapine: crystallization, solid-state characterization, and structural relationships. Cryst Growth Des. 2003;3:897–907.
24. Oliver WC, Pharr GM. Measurement of hardness and elastic modulus by instrumented nanoindentation: advances in understanding and refinements to methodology. J Mater Res. 2004;19:3–20.
25. Armstrong NA, Haines-Nutt RF. Elastic recovery and surface area changes in compacted powder systems. J Pharm Pharmacol. 1972;24: 135–6.
26. Triggle AM, Shefter E, Triggle DJ. Crystal structures of calcium channel antagonists: 2,6-dimethyl-3,5-dicarbomethoxy-4-[2-nitro-, 3-cyano-, 4-(dimethylamino)-, and 2,3,4,5,6-pentafluorophenyl]-1, 4-dihydropyridine. J Med Chem. 1980;23(12):1442–5.
27. Kojić-Prodić B, Ružić-Toroš Ž. Structure of the anti-inflammatory drug 4-hydroxy-2-methyl-N-2-pyridyl-2H-1λ^6, 2-benzothiazine-3-carboxamide 1,1-Dioxide (Piroxicam). Acta Cryst B. 1982;38: 2948–51.
28. Overgaard J, Hibbs DE. The experimental electron density in polymorphs A and B of the anti-ulcer drug famotidine. Acta Crystal A. 2004;60:480–7.
29. Bhardwaj RM, Price LS, Price SL, Reutzel-Edens SM, Miller GJ, Oswald IDH, *et al.* Exploring the experimental and computed crystal energy landscape of olanzapine. Cryst Growth Des. 2013;13:1602–17.
30. Lu J, Wang X, Yang X, Ching C. Characterization and selective crystallization of famotidine polymorphs. J Pharm Sci. 2007;96: 2457–68.
31. Lin SY, Cheng WT, Wang SL. Thermodynamic and kinetic characterization of polymorphic transformation of famotidine during grinding. Int J Pharm. 2006;318:86–91.

32. Roberts RJ, Rowe RC. The compaction of pharmaceutical and other model materials: a pragmatic approach. Chem Eng Sci. 1982;42: 903–11.
33. Anuar MS, Briscoe BJ. The elastic relaxation of starch tablets during ejection. Powder Technol. 2009;195:96–104.
34. Govedarica B, Ilić I, Šibanc R, Dreu R, Srčič S. The use of single particle mechanical properties for predicting the compressibility of pharmaceutical materials. Powder Technol. 2012;225:43–51.
35. Ilić I, Govedarica B, Šibanc R, Dreu R, Srčič S. Deformation properties of pharmaceutical excipients determined using an in-die and out-die method. Int J Pharm. 2013;446:6–15.
36. Shi L, Sun Changquan C. Transforming powder mechanical properties by core/shell structure: Compressible sand. J Pharm Sci. 2010;99:4458–62.
37. Ogienko AG, Boldyreva EV, Manakov AY, Boldyrev VV, Yunoshev AS, Ogienko AA, *et al.* A new method of producing monoclinic paracetamol suitable for direct compression. Pharm Res. 2011;28:3116–27.